Desalination and Water Treatment
www.deswater.com

doi: 10.5004/dwt.2021.27904

244 (2021) 291–301
December

Modelling and optimizing Orange G removal by heat-activated persulfate using two-step statistical strategies: Plackett–Burman and Box–Behnken designs

Naima Habache[a,b], Ouahiba Bechiri[a,*], Ilhem Djaghout[b,c], Meriem Djenouhet[d]

[a]*Laboratory of the Environmental Engineering, Department of the Process Engineering, Faculty of Engineering, University of Badji Mokhtar, Annaba, Algeria, emails: bechirio@yahoo.fr (O. Bechiri), naimahabache28@gmail.com (N. Habache)*

[b]*Department of the Process Engineering, Faculty of Science and Technology, University Mohamed-Cherif Messaadia, Souk Ahras, Algeria, email: i.djaghout@univ_soukaras.dz (I. Djaghout)*

[c]*Laboratory of Industrial Analysis and Materials Engineering, University 8 May 1945 of Guelma, Algeria*

[d]*Laboratory LOMOP, Department of the Process Engineering, Faculty of Engineering, University of Badji Mokhtar, Annaba, Algeria, email: djanomari@yahoo.fr*

Received 13 March 2021; Accepted 2 September 2021

ABSTRACT

In the treatment of water and wastewater, more emphasis is paid to the advanced oxidation process (AOP) based on ($S_2O_8^{2-}$) radicals. In this work, the degradation of a toxic dye (Orange G) using the heat-activated persulfate was examined Plackett and Burman designs experiments were used to investigate the effects of several parameters on the oxidation of the OG by $K_2S_2O_8$, including persulfate concentration $K_2S_2O_8$, the initial dye concentration, the reaction time, the initial solution pH, and temperature. The screening results identify three more influential factors that are subsequently studied by the response surface methodology employing Box–Behnken design to determine optimal conditions for maximal degradation effectiveness. The estimated values agreed with the experimental data, with a coefficient of the determination $R^2 = 0.9429$. The forecasted data revealed that with a concentration of Orange G 2 mg/L, a concentration of persulfates of 27.018 mM and a temperature of 45.5°C, a maximum orange degradation of 100% could be attained. The efficacy and the benefits of the advanced oxidation method using heat-activated persulfate for technological and industrial applications for the degradation of the organic pollutants have been well-proven in this work.

Keywords: Orange G; Persulfate heat-activation; Oxidation; Optimization; Plackett–Burman design; Box–Behnken design

1. Introduction

The wastewater of dyeing and finishing factories is a dangerous source of environmental contamination. The pollutants are characterized by high chemical and biochemical oxygen color concentrations of suspended solids' and so on. Reducing the color produced by residual dyes causes the most difficulties [1]. Thus, removing colors from industrial effluents before to release is a significant part of wastewater treatment and a serious environmental issue [2].

In the treatment of these dye-containing wastewaters, many traditional chemicals, physical, and biological methods have been employed, which are most commonly used because of their minimum environmental effects and economic efficiency [3], different chemical and physical processes are currently used, such as adsorption on an activated carbon, coagulation by chemical agents, ozone, or hypochlorite oxidation as well as electrochemical methods [2,4]. These methods do not totally eliminate colors, they can be costly, and usually generate additional

---

* Corresponding author.

This article was originally published with an error in the name of Meriem Djenouhet. This version has been corrected.
Please see Corrigendum in vol. 247 (2022) 319 [10.5004/dwt.2022.28275].

waste pollutants as secondary products [4,5]. The advanced oxidation processes (AOPS) are new methods for water treatment. They are widely used in the case of substances recalcitrant to conventional processes. These processes generate free hydroxyl radicals $HO^\bullet$ [Eq. (1)], which are highly effective in the degradation of organic pollutants due to their high oxidation capacity [5,6]:

$$HO^\bullet + H^+ + e^- \rightarrow H_2O \quad E^0 = 2.8V \tag{1}$$

The persulfate anion ($S_2O_8^{2-}$) is a strong and nonselective oxidant ($E° = 2.01$ V) equivalent to O_3 and H_2O_2, both of which are widely utilized in water and wastewater treatment [7,8]. The persulfate is increasingly utilized in the *in situ* chemical oxidation (ISCO) of soil, groundwater, or subsurface contamination, because of its relative stability at room temperature before activation [9,10]. It is a strong oxidizing agent but it kinetically is slow under ordinary conditions and it is frequently activated by heat [11], light ultrasound [12], or transition ions such as Fe(II) to generate an intermediate sulfate radical ($SO_4^{\bullet-}$, $E° = 2.6$ V) generalized by Eqs. (2) and (3), respectively [13,14].

$$S_2O_8^{2-} + \text{Heat} / \text{UV} \rightarrow 2SO_4^{\bullet-} \tag{2}$$

$$S_2O_8^{2-} + Me^{n+} \rightarrow Me^{n+} + SO_4^{\bullet-} + SO_4^{2-} \tag{3}$$

Among the above mentioned strategies, thermal treatment may be efficient in activating the persulfate and producing $SO_4^{2-\bullet}$ there upon considered as sustainable alternative for degrading a wide spectrum of the toxic organic contaminants for water and wastewater treatment applications [15]. Thermally activated PS has been found to provide a prominent alternative for the decomposition of many organic contaminants including chlorinated ethane, trichloroethanes, and BTEX compounds (benzene, toluene, ethylbenzene, and xylenes) [16–19]. This research is aimed in removing a toxic dye (Orange G) from an aqueous solution by thermal activation of PS. The Orange G (OG) is among the most often anionic dyes used in different fields such as: industries (Inks, photography, plastics, paper, and textiles), biological applications (detecting lung cancer metastasis, ophthalmic devices), and staining (adenohypophyseal cells, drinks, proteins, hairs, zeinic membranes, and urine sediments) [20].

This azo dye is toxic to the environment as well as human health, because it causes a variety of toxicities including acute oral toxicity, bacterial toxicity, carcinogenicity, chromosomal aberration, freshwater shrimp toxicity, genotoxicity, hematotoxicity, mutagenicity, serological toxicity, and short-term toxicity [20].

In order to minimize the number of tests and reduce the experiments, a popular class of screening designs (Placket–Burman design) was used. It was developed in 1946 by Plackett and Burman [21–23]. This method is a combination of statistical and mathematical techniques for creating experiments that allows create an experimental model and examine the effect each element individually and simultaneously in order to determine maximum degradation.

This method was applied to identify the parameters that affect the oxidation of the OG from an aqueous solution by a heat-activation PS.

The experimental results were statically analyzed, and a model of efficiency degradation based on operating conditions was carried out.

2. Materials and methods

2.1. Chemicals

Orange G ($C_{16}H_{10}N_2Na_2O_7S_2$), potassium persulfate ($K_2S_2O_8$), and sulfuric acid (H_2SO_4) were purchased from Sigma-Aldrich (American) and were used as receivers. Physicochemical characteristics of Orange G dye are listed

Table 1
Physical and chemical properties of Orange G dye

Common and commercial name	Orange G
Chemical/dye class	Azo
Molecular formula	$C_{16}H_{10}N_2Na_2O_7S_2$
Molecular weight (g/mol)	452.37
Physical form	Orange to red powder
Solubility	Soluble in water, methyl cellosolve; slightly soluble in ethanol; insoluble in xylene
Melting point	141°C
pH range	11.5–14.0
Color change	at pH Yellow (11.5) to pink (14.0)
pKa	12.8
Chemical structure	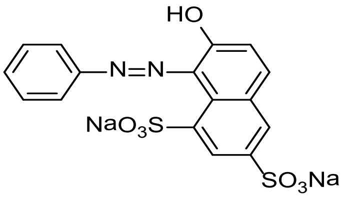

in Table 1 [24]. Sodium hydroxide (NaOH) was supplied by Biochem-Chimopharma (France). All the reagents used in the present study were purchased among the products of a high purity (analytical grade). All the experiments were carried out using distilled water.

2.2. Experimental procedures

An experimental device (batch reactor) a capacity of 500 mL was used to oxidizing Orange G by heat-activated persulfate. As a starting point for each manipulation, an OG solution at a concentration of (2–30 mg/L) was prepared from the dye stock solution (100 mg/L) for all the experiments, 100 mL of solution was used. Sulfuric acid (0.1 M H_2SO_4) or sodium hydroxide (0.1 M NaOH) were utilized to modify the pH of the solution to the required value (3 and 8).

A concentration of persulfate (3.7–29.6 mM) was added to the dye solution once the pH had been adjusted. A magnetic stirrer was used to homogenize the reaction mixture at a constant speed of 350 rpm. The treatment was carried out at temperatures between 30°C and 50°C for 40–90 min.

The degradation process of the azo day solution is based on the decrease in absorbance (A) at a maximum wave-length ($\lambda_{\max}$ = 482 nm) [25] of the OG measured using UV-Vis spectrophotometer Libra S6 Biochrom. The following equation [Eq. (4)] was used to obtain the degradation efficiency [26]:

$$\text{DE\%} = \frac{C_i - C_f}{C_i} \times 100 \tag{4}$$

where DE is the degradation efficiency, C_i is the initial dye concentration, and C_f is the final dye concentration.

3. Results and discussion

3.1. Screening design

The OG degradation was conducted by simultaneously altering five parameters listed in Table 2. The minimum and maximum levels for each factor were chosen after a literature review and, in particular, after performing the preliminary tests. Table 3 outlines the varied degradation operating conditions using heat activation PS based to a Placett–Burman design. Additionally, the experimental results of the efficiency degradation are presented. The degradation efficiency ranged from 2% to 100% at 25°C and 50°C, respectively, in the 12 tests. All the following statistical studies are based on these experimental data.

Table 2
Parameters and levels

Factor	Symbol	Unit	Level	
			Low (–1)	High (+1)
Persulfate concentration	[PS]	mM	3.7	29.6
Orange G concentration	[OG]	mg/L	2	30
Time	Time	Min	40	90
Initial pH	pH	–	3	8
Temperature	T	°C	25	50

3.1.1. Pareto chart

The Pareto effects diagram is used to identify the most important factors. The effects are standardized (F-value) for a better comparison. On the other hand, the standardized value is obtained by dividing factor's effect by error on the estimated value of the corresponding factor [27].

According to Fig. 1, the effect of the factors is significant if its F-value exceeds 2,447, whereas the selected confidence interval is 95%. It is found that temperature is the most important factor, since the generation of sulfate radicals increases with increasing temperature, persulfate concentration [PS] and orange G concentration [OG]. Whereas, time and pH are shown to be the least important factors.

3.1.2. Main effects

The factor's effect is defined as the change in reaction caused by a change in the factor's level [28]. Fig. 2 shows the main effects of the factors on degradation efficiency of orange G. Persulfate concentration and temperature have a positive effect on the reaction, however, pollutant concentration has a negative effect on degradation efficiency. Time and pH have a modest and favorable effect. The positive effect on the response shows that an increase in these factors implies an increase in the degradation efficiency of the orange G.

The degradation efficiency increases with increasing temperature, which is consistent with the previous study, and could be attributed to the generation of sulphate-based radicals at high temperatures [29,30]; the persulfate activated by the thermal energy generates $SO_4^{\bullet-}$ radicals, which participate in the oxidation reaction and degrades the organic pollutants. Thus, adding a higher initial concentration of persulfate to the system could produce more $SO_4^{\bullet-}$, boosting the degradation efficiency [31].

Table 3
Experimental results according to Plackett–Burman design

Run	[PS]	[OG]	Time	pH	T	DE (%)
1	3.7	2	40	3	25	19.56
2	29.6	2	40	3	50	100
3	29.6	2	90	3	25	63.84
4	3.7	30	90	8	25	5.85
5	3.7	30	40	3	25	2.94
6	29.6	2	90	8	25	73.17
7	3.7	2	40	8	50	100
8	29.6	30	40	8	50	77.57
9	29.6	30	90	3	50	99.58
10	3.7	2	90	8	50	100
11	29.6	30	40	8	25	4.58
12	3.7	30	90	3	50	46.76

As shown in Fig. 3, the rate of degradation process was found to be much less disturbed in presence of the hydroxide buffer, the basic medium slightly activates the generation of $SO_4^{\bullet-}$ sulfate radicals in pH 3 and 8, resulting in a slight increase in the degradation efficiency of the Orange G. However, the degradation efficiency of the Orange G was found to follow almost the same trend under all pH conditions studied, indicating that the impact of pH is very marginal and negligible [32].

The increase in pollutant concentration causes a decrease in degradation efficiency, which is explained by a significant and negative effect of orange G concentration on degradation efficiency. This phenomenon is explained by the fact that an increase in the initial dye concentration leads to an increase in the number of molecules of the orange G, while the number of persulfate radicals remains constant. Thus, causing a decrease in the kinetics of the degradation reaction as well as degradation efficiency [33].

3.1.3. Analysis of variance

Analysis of variance (ANOVA) compares the variances of the values calculated by the model and the residuals in order to absolutely test the influence of factors on the variations of a given response. If an effect is significant, there will be a high probability (95%, 99%, or 99.9%) that the effect is "real" [34–36]. The most important factors can be determined using a statistical parameter which is the *P*-value (Table 3). This value is compared by another value α which represents the risk of the model generally

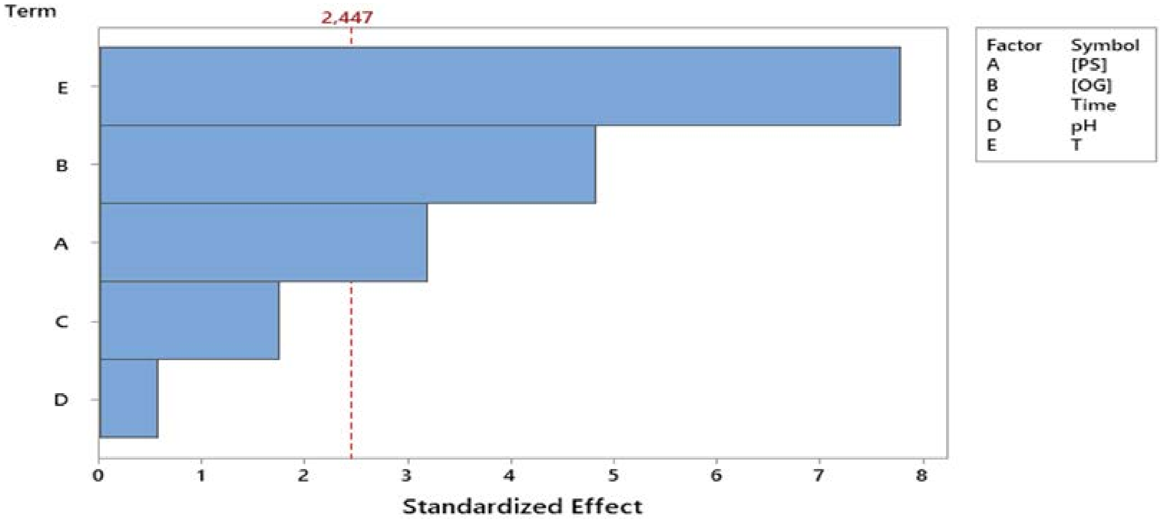

Fig. 1. Pareto-chart of the standardized effects for DE (%) as response (Alpha = 0.05).

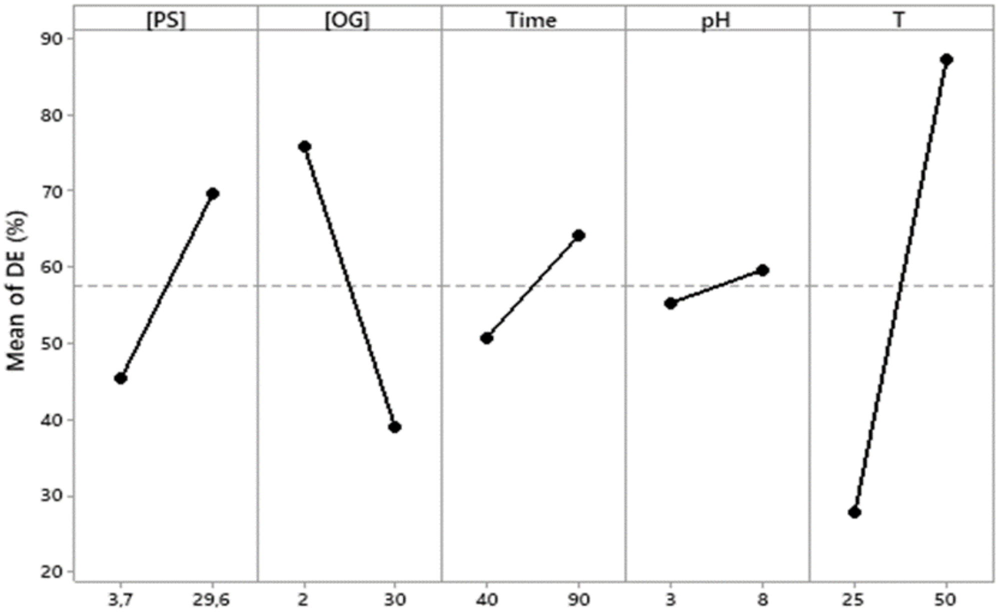

Fig. 2. Main effects plot of parameters for DE (%).

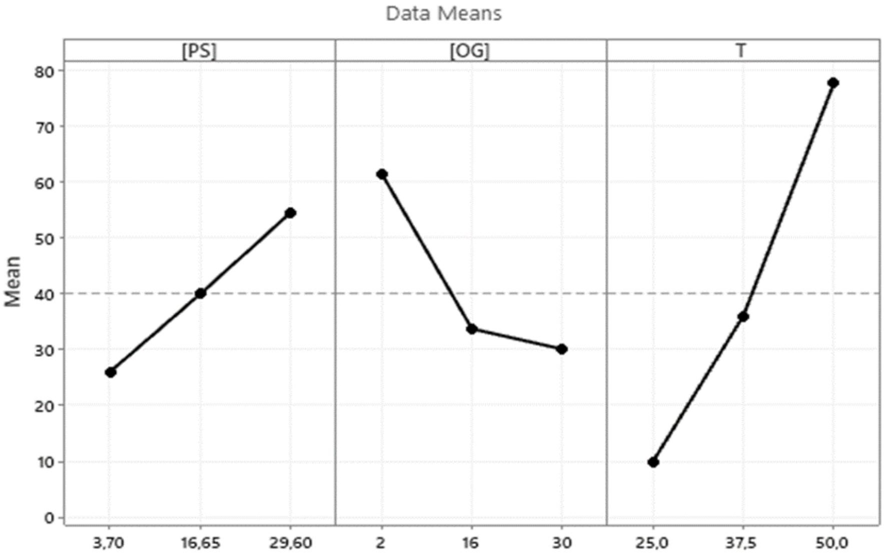

Fig. 3. Main effects plot of parameters for DE (%).

α is 5% risk. The coefficients of the parameters presented in Table 4. The algebraic coefficient values measure the average change in degradation efficiency as the parameters change from level (–1) to level (+1).

3.1.4. Polynomial regression

The experimental design method optimizes the response (the degradation efficiency) of the system, and represents it using a mathematical model that takes into account all the factors polynomial Eqs. (5) and (6) respectively, corresponding to the coded and non-coded parameters, are used to depict the regressions:

$$\text{ED} = 57.48 + 12.18[\text{PS}] - 18.48[\text{OG}] + 6.70\text{time} + 2.16\text{pH} + 2.84T \quad (5)$$

$$\text{ED} = -48.8 + 34.8[\text{PS}] - 1.32[\text{OG}] + 0.27\text{time} + 0.87\text{pH} + 2.39T \quad (6)$$

In addition, the comparison of estimated and measured responses (Table 5) shows a high coefficient of the determination $R^2 = 94.17\%$. It indicates a good correlation, which is confirmed by the adjusted R squared value ($R^2_{\text{adj}} = 89.32\%$).

3.2. Box–Behnken design

The Plackett–Burman experiment design is a first step to determine the most important operating parameters for the degradation of the orange G using the advanced oxidation technique. However, to improve the efficiency of this process an optimization of these parameters can be performed by the response surface methodology (RSM).

To improve the degradation efficiency, a second experimental design must be carried out using only the most important parameters. While the time is fixed at the minimum because the efficiency value is almost constant in the interval 40–90 min and the pH at a natural value since there is no significant difference between the degradation efficiency values at pH values 3 and 8 because at a pH close to neutral, the radical $SO_4^{-\bullet}$ is dominant [37]. A Box–Behnken design with three parameters becomes very useful for optimizing the degradation of the orange G. The effects of the

Table 4
Effects and coefficients of the estimated efficiency (coded units)

Term	Effect	Coeff	Coef ErT	*T*-value	*P*-value	FIV
Constant		57.48	3.84	14.97	0.000	
[PS]	24.36	12.18	3.84	3.17	0.019	1.00
[OG]	–36.97	–18.48	3.84	–4.81	0.003	1.00
Time	13.41	6.70	3.84	1.75	0.131	1.00
pH	4.33	2.17	3.84	0.56	0.593	1.00
T	59.68	29.84	3.48	7.77	0.000	1.00

Table 5
Comparison between estimated and experimental efficiency

Run order	DE_{exp} (%)	DE_{est} (%)
1	19.56	25.078
2	100.00	109.108
3	63.04	62.441
4	2.55	5.53
5	2.94	–11.686
6	73.17	67.170
7	100.00	89.084
8	77.56	76.474
9	99.58	85.553
10	100.00	102.493
11	4.58	16.798
12	46.76	61.199

parameters and their interactions have been studied in the same intervals of the screening Plackett–Burman design (Table 6).

Box–Behnken's design for three factors consisting of 15 trials experimental responses (ED %) is shown in Table 7. The data in this table will undergo a statistical processing to estimate the coefficients of the mathematical model.

3.2.1. Main effects plot and interactions for DE (%)

The findings of the function analysis using a Box–Behnken design demonstrate that all of the main effects are statistically significant (Fig. 3). The interaction diagram (Fig. 4) depicts the corrected mean of the degradation efficiency value vs. the persulfate concentration, orange G concentration, and temperature combinations. Because the lines in this picture are not all parallel, it implies that the link between the efficiency value and each element is dependent on the other factor. However, a Box–Behnken design function indicates that the effects of interactions of three parameters are not statistically significant, but the influence of temperature on degradation efficiency is stronger for the lowest and highest concentrations of persulfate and orange G.

The temperature of the reaction influences the link between the value of the degradation efficiency and the concentration of persulfate. When the temperature is set to 25°C, the degradation efficiency values for the three persulfate concentrations are nearly comparable. However, at 50°C, the concentration of persulfate is associated with significantly different and higher efficiency values. This finding is consistent with what has been observed in the literature [38].

Table 6
Process variables and levels in Box–Behnken design

Factor	Symbol	Unit	Levels		
			Low (–1)	Medium (0)	High (+1)
Persulfate concentration	[PS]	mM	3.7	16.65	29.6
Orange G concentration	[OG]	mg/L	2	16	30
Temperature	T	°C	25	37.5	50

In the instance of Orange G concentration, the degradation efficiency at 25°C is nearly same in the three Orange G concentrations. However, increasing the temperature to 50°C enhances the efficiency values, especially when the Orange G concentration is equal to 2 mg/L. This finding is congruent with that of Gu et al. [39].

3.2.2. Statistical results and the interpretation

Calculation of regression coefficients with coded data is provided by MINITAB version 19 software (Table 8).

P-value was used as a statistical indicator to assess which terms in the model are significant. According to

Table 7
Box–Behnken plan with experimental responses

Run order	[PS]	[OG]	T	DE_{exp} (%)	DE_{est} (%)
1	3.7	2	37.5	47.77	39.11
2	29.6	2	37.5	88.63	76.82
3	3.7	30	37.5	5.11	16.92
4	29.6	30	37.5	27.55	36.20
5	3.7	16	25	2.82	1.53
6	29.6	16	25	5.48	7.34
7	3.7	16	50	48.28	46.42
8	29.6	16	50	96.27	97.85
9	16.65	2	25	26.53	36.48
10	16.65	30	25	4.89	–5.63
11	16.65	2	50	82.82	93.34
12	16.65	30	50	82.59	72.464
13	16.65	16	37.5	29.44	27.60
14	16.65	16	37.5	27.31	27.60
15	16.65	16	37.5	26.06	27.60

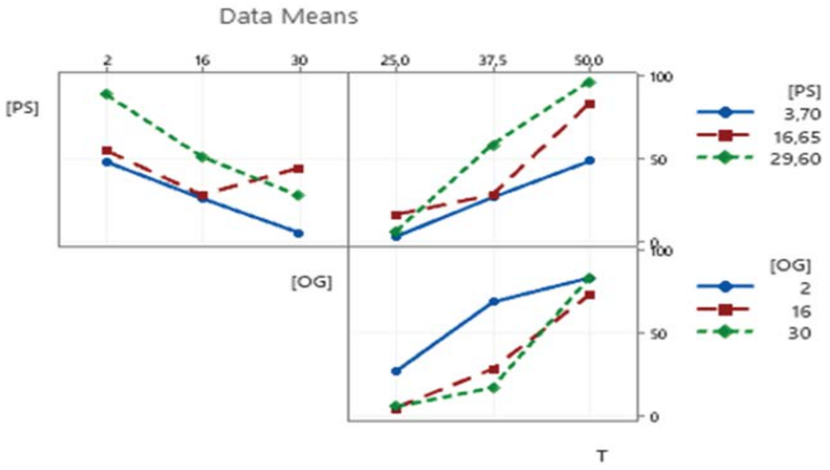

Fig. 4. Diagram of interactions for DE %.

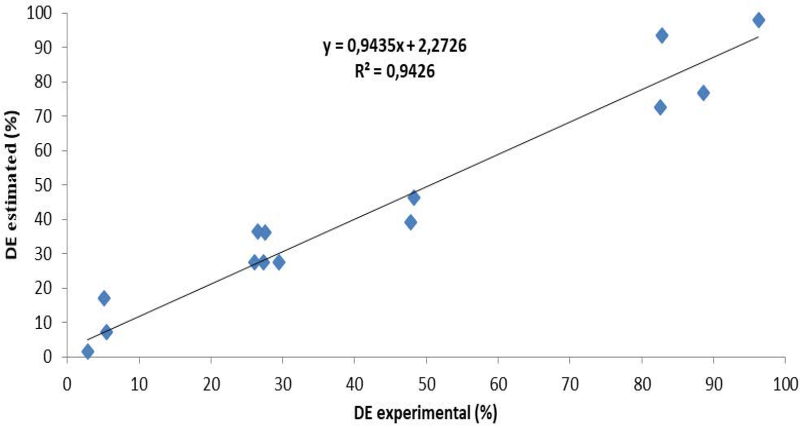

Fig. 5. Plot of experimental vs. predicted values of the degradation efficiency DE (%).

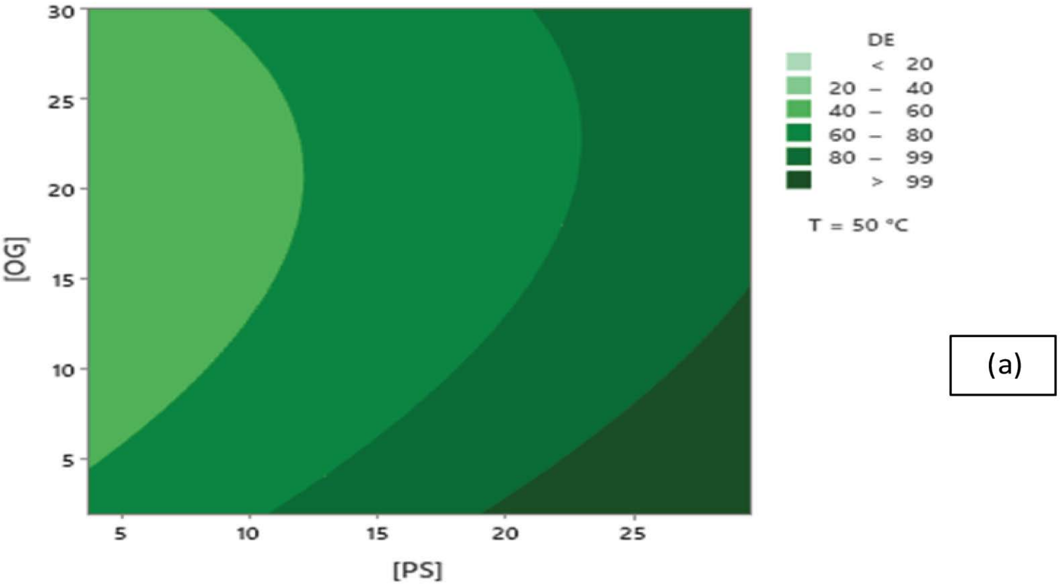

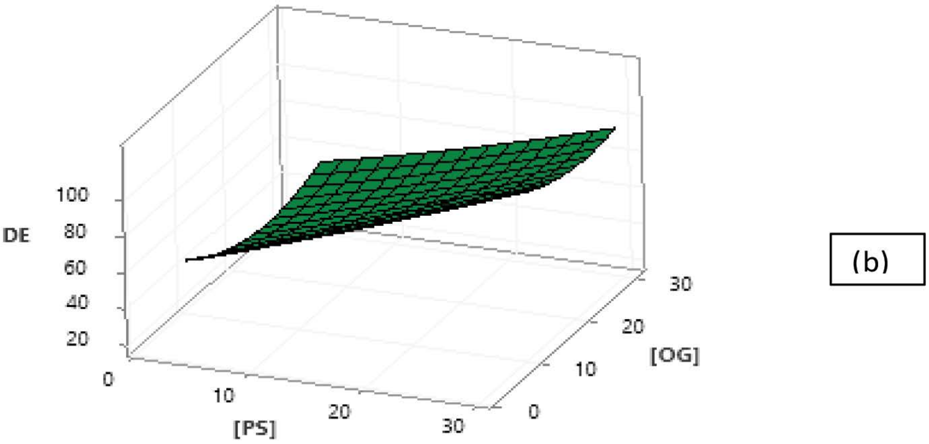

Fig. 6. Contour plots (a) and response surface (b) of the degradation efficiency according [OG] and [PS] at high levels of T.

Table 8
Regression coefficients estimated for efficiency DE (%)

Term	Coeff	Er *T* coeff	*T*-value	*P*-value	Fiv
Constant	27.60	7.59	3.64	0.015	
[PS]	14.25	4.65	3.06	0.028	1.00
[OG]	–15.70	4.65	–3.38	0.02	1.00
T	33.78	4.65	7.27	0.001	1.00
[PS] × [PS]	1.84	6.84	0.27	0.79	1.01
[OG] × [OG]	12.83	6.84	1.87	0.12	1.01
T × T	8.78	6.84	1.28	0.25	1.01
[PS] × [OG]	–4.60	6.57	–0.70	0.51	1.00
[PS] × T	11.34	6.57	1.72	0.14	1.00
[OG] × T	5.35	6.57	0.81	0.45	1.00

R^2 = 94.29% and R^2_{adj} = 84.01%

ANOVA (Table 8), the value of $P = 0.000$ indicates that the model is significant. On the other hand, the set of linear effects with the value of $P = 0.015$ (<0.05) indicates that there is a significant linear effect as well as for the main factors; [PS], [OG], and T.

The model contains three squared effects: persulfate concentration, Orange G concentration, and temperature. The *P*-values for each of the squared effects are greater than 0.05. As a result, there is no significant effect, that is, the degradation efficiency does not change when the square effect of the three factors is varied, and we do not expect any curvature in the response surfaces.

3.2.3. Determination of the mathematical model

The polynomial regression equation for the primary model (before excluding non-significant terms), is written as follows:

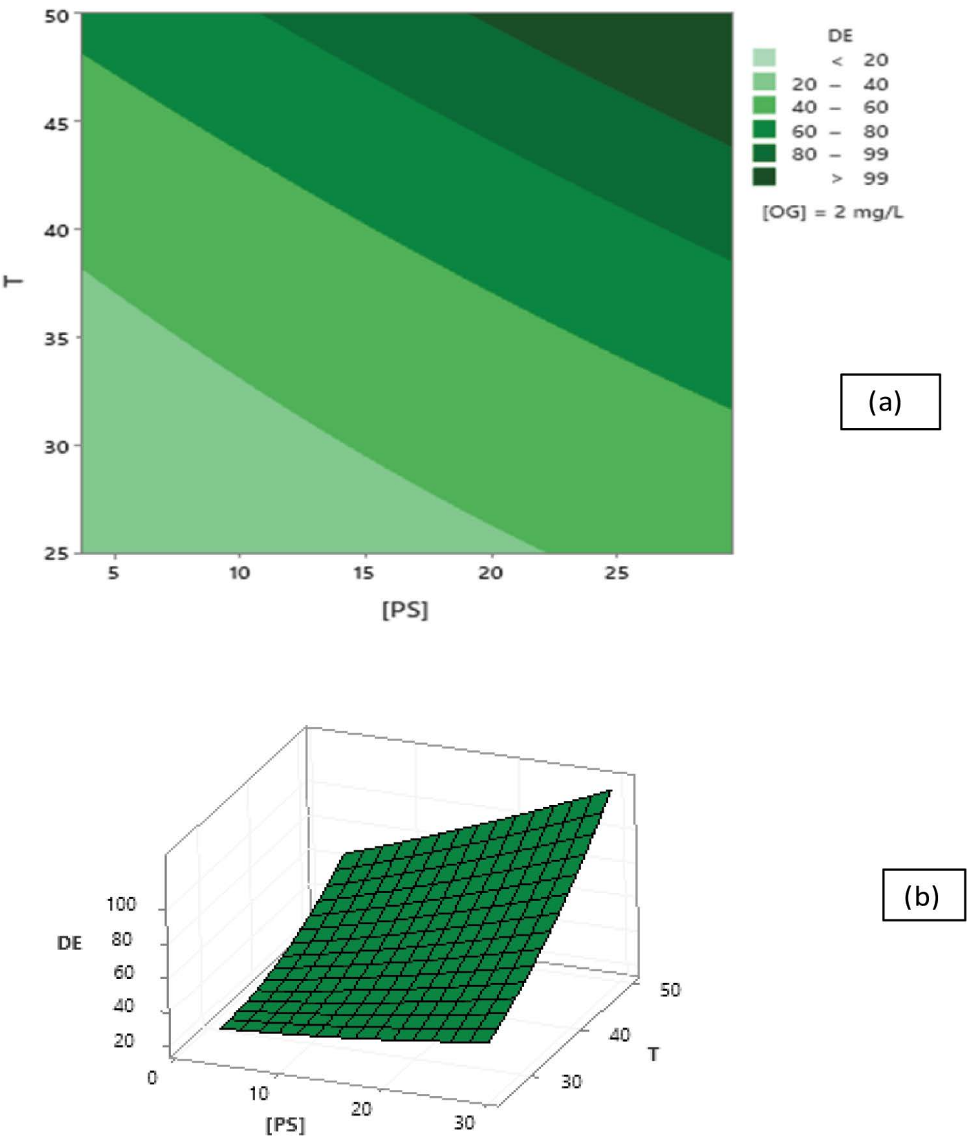

Fig. 7. Contour plots (a) and response surface (b) of the degradation efficiency according *T* and [PS] at low levels of [OG].

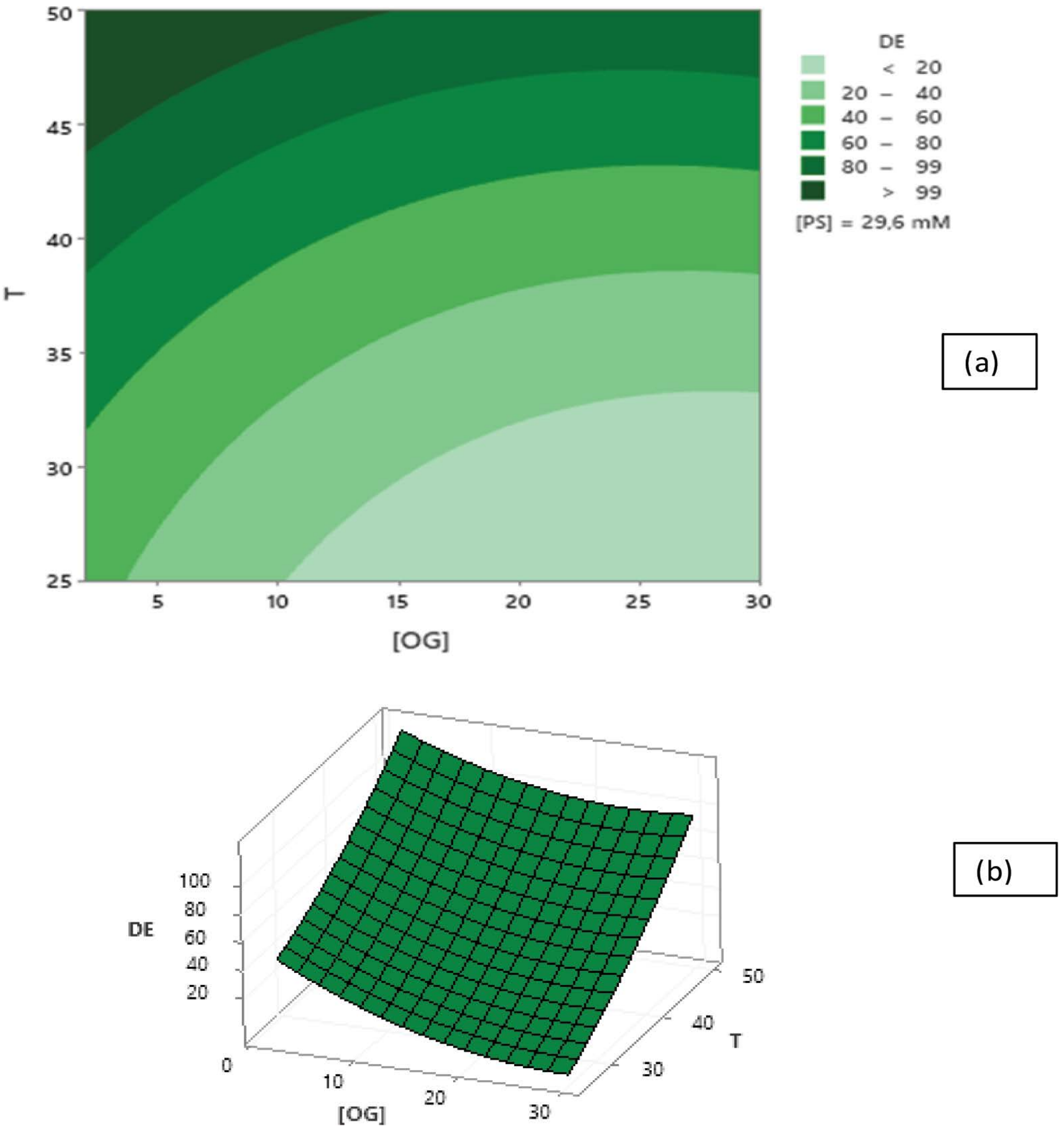

Fig. 8. Contour plots (a) and response surface (b) of the degradation efficiency according *T* and [OG] at high levels of [PS].

Coded units:

$$\begin{aligned}\text{ED} = {} & 27.60 + 14.25[\text{PS}] - 15.70[\text{OG}] + 33.78T \\ & + 1.84[\text{PS}] \times [\text{PS}] + 12.3[\text{OG}] \times [\text{OG}] \\ & + 8.78T \times T - 4.60[\text{PS}] \times [\text{OG}] + 11.34[\text{PS}] \times T \\ & + 5.35[\text{OG}] \times T \end{aligned} \tag{7}$$

Uncoded units:

$$\begin{aligned}\text{DE} = {} & 80 - 1.48[\text{PS}] - 3.94[\text{OG}] - 3.17T \\ & + 0.01[\text{PS}] \times [\text{PS}] + 0.06[\text{OG}] \times [\text{OG}] \\ & + 0.05T \times T - 0.02[\text{PS}] \times [\text{OG}] + 0.07[\text{PS}] \times T \\ & + 0.03[\text{OG}] \times T \end{aligned} \tag{8}$$

The correlation can also be demonstrated by graphing the measured responses vs. the estimated responses. This may be shown in Fig. 5, which reveals a high association between the two. The points in Fig. 5 are spread around the regression line. Since a result, the model is of sufficient quality, as there is a 94.26% probability that it explains the measured changes in response. For the phenomenon under study, the model provides an adequate description.

3.2.4. Contour plots and the response surface

The final stage is to determine the values of the parameters that result in the best answer [40]. Using the approved mathematical model and Minitab 19. There are two kinds of response surface plots: contour plots and surface plots. These plots depict the relationships between a response variable and two factors in an equation model while holding

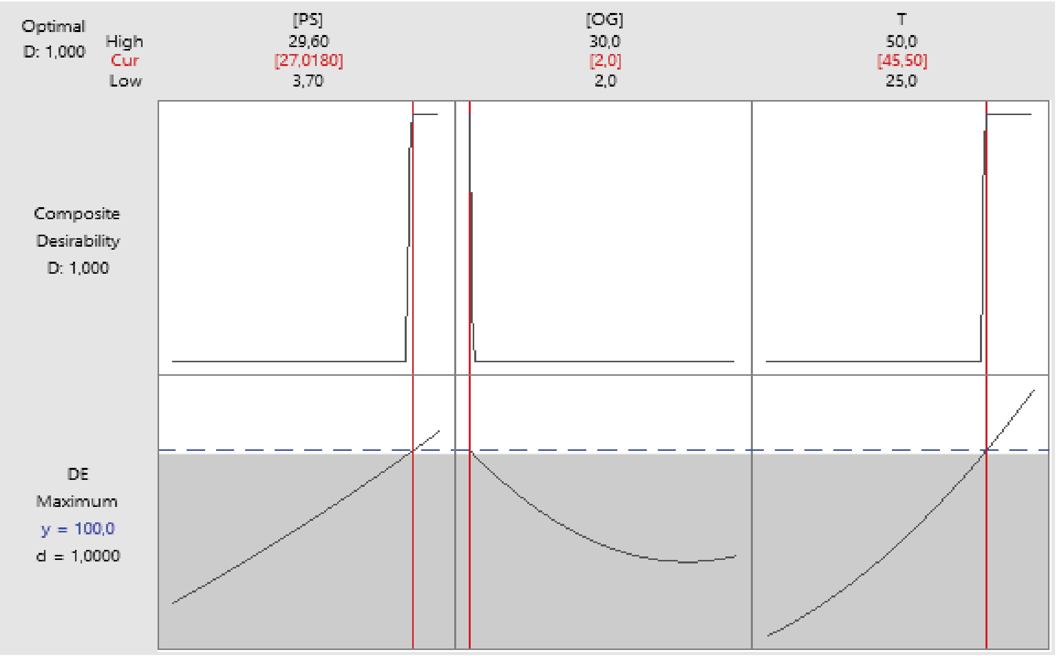

Fig. 9. Optimization response for degradation the Orange G at 2 mg/L.

Table 9
Optimum predicted values of the factor for the maximum degradation efficiency

[OG]	[PS]	*T*	DE pred (%)	DE exp(%)
2	27.018	45.5	100	100

the possible extra factors constant. They also specified the desired response values and operational circumstances. The orientation of the response surface altered with the levels of the operational parameter values of persulfate concentration, Orange G concentration, and temperature, as note un this representation. The greatest degradation efficiency was likewise obtained at *T* = 50°C (Fig. 6), Orange G concentration of 2 mg/L (Fig. 7), and persulfate concentration of 29.6 mM (Figs. 7 and 8).

3.2.5. Optimization and model validation

Optimization consists in finding the optimal experimental conditions corresponding to a maximum of the degradation efficiency. And to target the experimental field for the best response, an optimization was applied. The results of the optimization indicate the optimal values for each factor and the optimal value of the degradation efficiency. A constraint was imposed on [PS], [OG], and T. The experimental design can also be used to search for an optimum. Table 9 summarizes the best values for Orange G degradation efficiency, as well as their optimal operating conditions.

From Fig. 9, the degradation efficiency could be obtained with a value of 100%. The desirability is equal to 1, and when the desirability is high, that is, close to 1, the response is better and closer to the desired value.

From the theoretical model, the degradation efficiency can be obtained with a value of 100% with optimized values of all parameters. A check of the optimal conditions was performed twice under the same experimental conditions; the degradation of Orange G was performed with 100% efficiencies. Thus, the model was sufficient to represent the process.

4. Conclusions

This study comprehensively studied the Orange G removal performance utilizing thermally activated persulfate oxidation by considering a variety of influencing parameters such as, persulfate concentration, initial Orange G concentration, the reaction time, the initial solution pH, and the temperature, using the Plackett–Burman and the Box–Benhken designs. The degradation of the Orange G was carried out while adjusting several operator parameters at the same time. The most critical criteria for the degradation efficiency of the OG were the persulfate concentration, the initial Orange G concentration, and the temperature. It was proven by the RSM method based on the Box–Behnken design that persulfate, Orange G, and temperature have substantial effects, which had already been explored by the Placett–Burman design.

Consequently, a persulfate concentration of 27.018 mM and a temperature of 45.5°C resulted in 100% degradation of Orange G (2 mg/L). These results inspired us to utilize the new oxidation method employing heat-activated persulfate for technological and industrial applications since we achieve maximum efficiency with the least quantity of consumption.

References

[1] E.G. Solozhenko, N.M. Soboleva, V.V. Goncharuk, Decolorization of azo dye solutions by Fenton's oxidation, Water Res., 29 (1995) 2206–2210.

[2] O. Legrini, E. Oliveros, A.M. Braun, Photochemical processes for water treatment, Chem. Rev., 93 (1993) 671–698.

[3] Y. Peng, D. Fu, R. Liu, F. Zhang, X. Liang, $NaNO_2/FeCl_3$ catalyzed wet oxidation of the azo dye Acid Orange 7, Chemosphere, 71 (2008) 990–997.

[4] O. Bechiri, M. Abbessi, M.E. Samar, Decolorization of organic dye (NBB) using Fe(III) $P_2W_{12}Mo_5/H_2O_2$ system, Desal. Water Treat., 51 (2013) 31–33.

[5] O. Bechiri, M. Abbessi, L. Ouahab, The oxidation study of methyl orange dye by hydrogen peroxide using Dawson-type heteropolyanions as catalysts, Res. Chem. Intermed., 39 (2013) 2945–2954, doi: 10.1007/s11164-012-0807-3.

[6] K.H. Chan, W. Chu, Modeling the reaction kinetics of Fenton's process on the removal of atrazine, Chemosphere, 51 (2003) 305–311.

[7] P. Wardman, Reduction potentials of one-electron couples involving free-radicals in aqueous solution, J. Phys. Chem. Ref. Data, 18 (1989) 1637–1755.

[8] Y.G. Adewuyi, Sonochemistry in environmental remediation; combinative and hybrid sonophotochemical oxidation processes for the treatment of pollutants in water, Environ. Sci. Technol., 39 (2005) 3409–3420.

[9] S.G. Huling, B.E. Pivetz, *In-situ* Chemical Oxidation, DTIC Document, 2006, EPA/600/R-06/072.

[10] R.L. Siegrist, M. Crimi, T.J. Simpkin, The Interstate Technology and Regulatory Council (ITRC), *In Situ* Chemical Oxidation of Contaminated Soil and Groundwater, $ISCO_2$, Springer, London, 2005.

[11] Y. Chen, P. Deng, P. Xie, R. Shang, Z. Wang, S. Wang, Heat-activated persulfate oxidation of methyl- and ethyl-parabens: effect, kinetics, and mechanism, Chemosphere, 168 (2017) 1628–1636.

[12] X. Wang, L. Wang, J. Li, J. Qiu, C. Cai, H. Zhang, Degradation of Acid Orange 7 by persulfate activated with zero valent iron in the presence of ultrasonic irradiation, Sep. Purif. Technol., 122 (2014) 41–46.

[13] C. Liang, H.W. Su, Identification of sulfate and hydroxyl radicals in thermally activated persulfate, Ind. Eng. Chem. Res., 48 (2009) 5558–5562.

[14] C. Liang, I. Lee, I. Hsu, C.P. Liang, Y.L. Lin, Persulfate oxidation of trichloroethylene with and without iron activation in porous media, Chemosphere, 70 (2008) 426–435.

[15] X. Chen, M. Murugananthan, Y. Zhang, Degradation of p-Nitrophenol by thermally activated persulfate in soil system, Chem. Eng. J., 283 (2016) 1357–1365.

[16] L. Eberson, E. Mikael, Electron Transfer Reactions in Organic Chemistry.XI;The reaction between carbon tetrabromide and the cage comples [Co(II) sepulchrate]$^{2+}$: Ainitic and product study, Acta. Chem. Scand., B41 (1987) 41–49.

[17] C.J. Liang, C.J. Bruell, M.C. Marley, K.L. Sperry, Thermally activated persulfate oxidation of trichloroethylene (TCE) and 1,1,1trichloroethane (TCA) in aqueous systems and soil slurries, Soil. Sediment Contam., 12 (2003) 207–228.

[18] K.C. Huang, Z.Q. Zhao, G.E. Hoag, A. Dahmani, P.A. Block, Degradation of volatile organic compounds with thermally activated persulfate oxidation, Chemosphere, 61 (2005) 551–560.

[19] C.J. Liang, C.F. Huang, Y.J. Chen, Potential for activated persulfate degradation of BTEX contamination, Water Res., 42 (2008) 4091–4100.

[20] R.W. Sabnis, Hand Book of Biological Dyes and Stains; Synthesis and Industrial Applications, John Wiley and Sons, Inc., Canada, 2010.

[21] R. Phan-Tan-Luu, D. Mathieu, Planification D'expérience en Formulation: Criblage [Experimental Design in Formulation: Screening], Techniques de L'ingénieur, Paris, 2008, J2240, pp. 1–13.

[22] E.B. Dean, Taguchi Approach to Design Optimization for Quality and Cost, Annual Conference of the International Society of Parametric Analysts, 1991.

[23] R.L. Plackett, J.P. Burman, The design of optimum multifactorial experiments, Biometrika, 33 (1946) 305–325.

[24] National Center for Biotechnology Information, Pub Chem Compound Summary for CID 16015, Orange G, 2020.

[25] M. Lounis, M.E. Samar, O. Hamdaoui, Sono-electrochemical degradation of Orange G in pure water, natural water, and seawater: effect of operating parameters, Desal. Water Treat., 57 (2015) 22533–22542.

[26] G. Burgot, J.-L. Burgot, Méthodes Instrumentales D'analyse Chimique et Applications: Méthodes Chromatographiques, Électrophorèses, Méthodes Spectrales et Méthodes Thermiques, French, 3rd Edn., 2011, p. 227.

[27] H. Aouici, H. Bouchelaghem, M.A. Yallese, M. Elbah, B. Fnides, Machinability investigation in hard turning of AISI D3 cold work steel with ceramic tool using response surface methodology, Int. J. Adv. Manuf. Technol., 73 (2014) 1775–1788.

[28] I. Djaghout, A.M. Affoune, M.L. Chelaghmia, M. Bendjaballah, Experimental investigation of nickel electrodeposits brightness in the presence of surfactants: modeling, optimization and polarization studies, Port. Electrochim. Acta, 33 (2015) 209–222.

[29] Y. Ji, C. Dong, D. Kong, J. Lu, Q. Zhou, Heat-activated persulfate oxidation of atrazine: implications for remediation of groundwater contaminated by herbicides, Chem. Eng. J., 263 (2015) 45–54.

[30] J. Deng, Y. Shao, N. Gao, Y. Deng, S. Zhou, X. Hu, Thermally activated persulfate (TAP) oxidation of antiepileptic drug carbamazepine in water, Chem. Eng. J., 228 (2013) 765–771.

[31] Y.F. Rao, L. Qu, H. Yang, W. Chu, Degradation of carbamazepine by Fe(II)-activated persulfate process, J. Hazard. Mater., 268 (2014) 23–32.

[32] C. Tan, N. Gao, Y. Deng, N. An, J. Deng, Heat-activated persulfate oxidation of Diuron in water, Chem. Eng. J., 203 (2012) 294–300.

[33] L. Loukas, A Placket–Burman screening design directs the efficient formulation of multicomponent DRV liposomes, J. Pharm. Biomed. Anal., 26 (2001) 255–263.

[34] T.P. Ryan, Statistical Methods for Quality Improvement, Wiley, New York, NY, 1989.

[35] J. Goupy, What kind of experimental design for finding and checking robustness of analytical methods?, Anal. Chim. Acta, 544 (2005) 184–190.

[36] S. Norzaee, M. Taghavi, B. Djahed, F. Kord Mostafapour, Degradation of Penicillin G by heat activated persulfate in aqueous Solution, J. Environ. Manage., 215 (2018) 316–323.

[37] L. Liu, S. Lin, W. Zhang, U. Farooq, G. Shen, S. Hu, Kinetic and mechanistic investigations of the degradation of sulfachloropyridazine in heat-activated persulfate oxidation process, Chem. Eng. J., 346 (2018) 515–524.

[38] X. Gu, S. Lu, L. Li, Z. Qiu, Q. Sui, K. Lin, Q. Luo, Oxidation of 1,1,1-trichloroethane stimulated by thermally activated persulfate, Ind. Eng. Chem. Res., 50 (2011) 11029–11036.

[39] M.A. Bezerraa, R.E. Santelli, E.P. Oliveira, L.S. Villar, L.A. Escaleira, Response surface methodology (RSM) as a tool for optimization in analytical chemistry, Talanta, 76 (2008) 965–977.